Synchronization of Coupled Nonlinear Oscillators with Applications to Photonic Arrays

Banu Zharas

Master of Science Thesis in Applied mathematics

Department of Mathematics, School of Science and Technology
Nazarbayev University
Astana 010000, Kazakhstan
banu.zharas@nu.edu.kz

MSc Thesis Supervisor: Professor Anastasios Bountis

Members of Examination Committee:

Assist. Prof. Ardak Kashkynbaev
Department of Mathematics
School of Science and Technology
Nazarbayev University

Dr. Vassilios Basios Center of Nonlinear Phenomena and Complex Systems
Université Libre de Bruxelles
Brussels, Belgium

DEPARTMENT OF MATHEMATICS, NAZARBAYEV UNIVERSITY
KABANBAY-BATYR 53, NUR-SULTAN, 010000, REPUBLIC OF KAZAKHSTAN
MAY 2019

Abstract

In recent years, the study of synchronization of coupled oscillators have been the subject of intense research interest, leading to many new and unexpected phenomena. Our research is first focused on the analysis of a network of coupled nonlinear oscillators exhibiting the breakdown of synchronization into fascinating "chimera states" exhibiting the coexistence of synchronized and unsynchronized parts. We then apply these ideas to laser arrays of photonic "oscillators", which have numerous applications in optical communications, sensing and imaging. First of all, we demonstrate the occurrence of synchronization and chimera states in a simpler problem, consisting of a ring of coupled 4D simplified Lorenz systems, in which each oscillator is described by a Li-Sprott oscillator [1]. An interesting feature of each oscillator is the coexistence of a limit cycle and two symmetric strange attractors for some specific range of parameters, which influences the global synchronization dynamics and leads to the formation of chimera states. Inspired by this model, we study some fascinating oscillatory phenomena of coupled photonic oscillators consisting of dimers of semiconductor lasers, each of which is capable of performing limit cycle oscillations. Coupling in an appropriate way a large number of dimers in long arrays we find that they can exhibit combinations of oscillatory patterns involving long amplitude oscillations (LAO) and also localized oscillations of very small amplitude close to the fixed points (LOCFP). As preliminary results of this investigation, we show the coexistence of LOA and LOCFP patterns reminiscent of "chimera–like" states and LOCFP "breather–like" phenomena. Both of these behaviors are shown to be spatially robust, when we calculate the Discrete Laplacian of their amplitudes for long times.

ACKNOWLEDGEMENTS

During this research, I had several collaborations with several members of Prof. A. Bountis research team to make my work more efficient. Professor Bountis shared his valuable experience and regularly discussed with master students under his guidance the derivations and every time helped to turn to the next stage. Moreover, international collaborators helped me better understand the tasks involved in this project like Dr. Vasileios Basios and Prof. Yannis Kominis, Joniald Shena, faculty members of Université Libre de Bruxelles, Athens National Technical University and Russian National University of Science and Technology MISiS respectively. They taught me how to construct and implement Matlab codes for such tasks. In order to obtain initial results there were some collaborative works with Fatemeh Parestesh from Amirkabir University of Technology. Also, I would like to emphasize the help of studies during second Summer School of Kazakhstan on "Mathematical Methods in Science and Technology", which held on May 28-June 8, 2018, at the campus of the Al Farabi Kazakh National University in Almaty.

CONTENTS

I. Introduction

Everything around us is in constant motion. Nature does not often rest at an equilibrium state but prefers to execute oscillatory motion whereby major phenomena like daily changes and seasons occur periodically. If we look carefully, we notice a lot of interesting oscillatory phenomena taking place around us. They are not only explicit processes like evaporation of water, planetary motion, but even sleeping behavior of birds, dolphins and other mammals. In the latter case, these phenomena concern the synchronization of coupled systems, which may sometimes lead to the formation of fascinating *chimera states* of mixed synchronous and asynchronous behavior that is being studied by many scientists around the world for nearly 20 years.

Before studying synchronization in the dynamics of coupled nonlinear oscillators, we need to understand some of the relevant terms used in the international scientific literature and appreciate their importance in real-life applications:
What is an oscillatory object?
What is dynamics?
What is chaos?
What is interaction of nonlinear systems?
Only after establishing correct answers to above questions, we can turn to the study of synchronization in nonlinear systems.

Many physical phenomena are caused by the oscillatory behavior of *systems*, consisting of groups of coupled oscillators described by nonlinear ordinary differential equations (NODEs). Although the best known example is the motion of planetary systems, even individual cells and neurons oscillate and help vital systems of our body, like our heart and our brain, perform synchronized oscillations that are crucial for our life.

We are not interested here in the particular design of such mechanisms, but in their behavior in time. *Dynamics*, i.e. the study of their motion, helps us to investigate this behavior, through the solution of the NODEs that describe it. It signifies the development in time of the process of a body or a system, depending on some external factors. For example, some systems like the solar system may exhibit periodic motion, while others, like the weather, may demonstrate unpredictable behavior in time, attracting considerable attention to their *chaotic* dynamics.

How can we describe real life phenomena mathematically? How can we construct an appropriate mathematical model?

Differential equations describe the evolution of systems in continuous time [1], and thus are able to represent a wide variety of dynamical systems. While it is easy to solve analytically systems of *linear* ODEs, containing only first order terms in their dependent variables and find their general solutions using superposition principles, real life phenomena are difficult to analyze because they require understanding and dealing with *non-linearity*.

One important subset of the wide class of nonlinear dynamical systems is the one referring to *self-sustained oscillators* [2]. The concept of self-sustained oscillations is extremely important for an adequate description of many natural phenomena, and of synchronization in particular. Here we briefly summarize the properties of self-sustained oscillatory systems: Every oscillator is an active element and many such elements coupled together form a *system*. Each element contains an internal source of energy that is being constantly transformed into oscillatory movement.

Being isolated, the oscillator continues to generate the same rhythm until the source of energy expires. Mathematically, it is described by an autonomous (i.e., without explicit time dependence) set of NODEs, or a *dynamical system* for short. The main property of such oscillators is that they continue following their own rhythms when they are isolated. These rhythms are entirely determined by the properties of the systems themselves and are maintained due to the internal source of energy that compensates the *dissipation* present in the system.

Macroscopic natural systems generally dissipate their energy. This happens due to mechanical friction, as in the case of the oscillations of a suspended simple pendulum, or due to electrical

resistance in an oscillating electrical circuit, or due to other mechanisms of irreversible transformation of the system's energy into heat. Thus, excluding from our consideration examples such as planetary systems, where the dissipation is negligible, we always take into account the fact that, without a constant supply of energy into the system, its oscillations will eventually decay.

As a conclusion, therefore, self-sustained oscillators must possess an internal energy source [2]. Perhaps the most important and noteworthy example demonstrating the stability property of self sustained oscillators is our heart, which is stable to (at least small) perturbations caused by every day's unexpected changes of events. After these changes subside, the oscillations soon return to their original rhythm. Self-sustained oscillators are exhibited by rhythms of various shapes. Let us quantify such rhythms using the simple example of a pendulum clock. As is well known from classical mechanics, the differential equation (NODE) which represents the motion of a simple pendulum is [1]

$$\ddot{\theta} + \frac{g}{l}\sin\theta = 0 \tag{1}$$

where g is acceleration due to gravity, l is the length of the pendulum, and θ is the angular displacement. The above differential equation is not easily solved, since it is nonlinear, and its solution cannot be written in terms of elementary trigonometric functions. However, adding a restriction to the size of the oscillation's amplitude gives a form whose solution can be easily obtained. If it is assumed that the angle of oscillations is very small, i.e.

$$\theta << 1,$$

substituting for $\sin\theta$ into (1), using the small-angle approximation,

$$\sin\theta \approx \theta$$

yields the equation for a harmonic oscillator:

$$\ddot{\theta} + \tfrac{g}{l}\theta = 0.$$

The oscillation of the pendulum is now described by trigonometric functions (Figure 1), whose period $T = 2\pi\sqrt{l/g}$ is the main characteristic of the clock. Indeed, the mechanism that rotates the hands actually counts the number of pendulum oscillations, so that its period constitutes the basic time unit of the system.

Often it is convenient to characterize the rhythm by the number of oscillation cycles per time unit, or by the oscillation cyclic frequency

$$f = \frac{1}{T}. \tag{2}$$

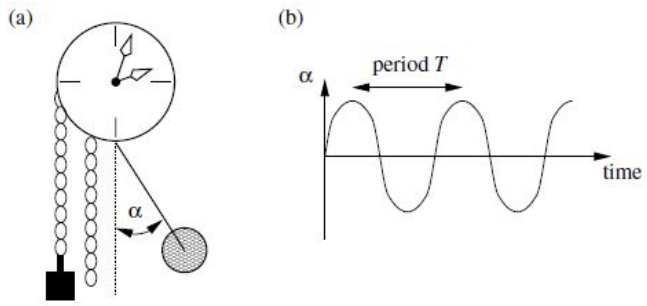

Fig. 1. (a) An example of a self-sustained oscillator, the pendulum clock. The potential energy of the lifted weight is transformed into oscillatory motion of the pendulum and can even lead to the rotation of hands. (b) For small angles, the motion of the pendulum is periodic, i.e., its angle with respect to the vertical varies in time with the period T.

Now, a single oscillating system such as a simple pendulum can be described by only its frequency and period. In order to understand, however, the interaction of two oscillating systems, we need to consider two *coupled* non-identical clocks. Experiments show that even a weak interaction can

synchronize these two clocks. That is, two clocks which, if taken apart, have different oscillation periods, when coupled adjust their rhythms and start to oscillate with a common period. [2], [3]

This phenomenon is often described in terms of coincidence of frequencies or frequency *locking* if two non-identical oscillators having their own frequencies f_1 and f_2 are coupled together, they start to oscillate with a common frequency. We measure how weak or strong the interaction is between oscillators by the strength of *their coupling*. If two oscillators are not connected, we say that coupling strength is equal to zero.

Frequency *detuning* or *mismatch* $f = f_1 - f_2$ quantifies how different the uncoupled oscillators are. If the mismatch of autonomous systems is not very large, the frequencies of the two clocks (in the coupled system) become equal, or *entrained*, whence we conclude that *synchronization* has taken place [2], [3].

Another, key point of synchronization theory pertains to the *phase* of an oscillator. The phase seems to provide no new information about the system, but its advantage becomes evident if we consider the difference of the phases of two clocks. This helps us to distinguish between two different synchronous regimes (see Figure 2).

Thus, if two pendula move in the same direction and almost simultaneously attain, say, the right-most position, then their phases ϕ_1 and ϕ_2 are close and this state is called *in-phase synchronization.* (Figure 2a). If the pendula of two synchronized clocks move in opposite directions then one speaks of synchronization in *anti-phase* (Figure 2b).

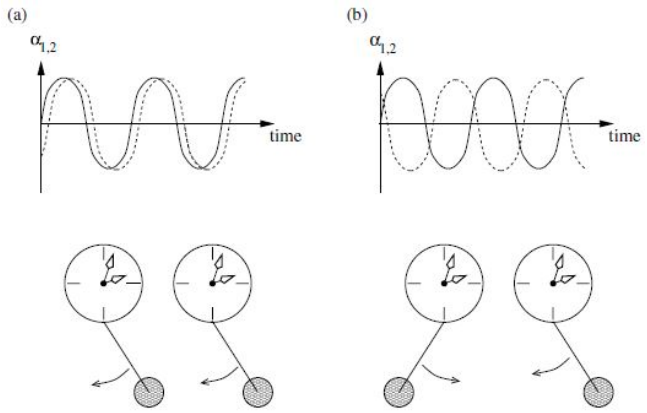

Fig. 2. Possible synchronous regimes of two nearly identical clocks: they may be synchronized almost in-phase (a), i.e., with the phase difference $\phi_2 - \phi_1 \approx 0$, or in anti-phase (b), when $\phi_2 - \phi_1 \approx \pi$

The onset of a certain *synchronous* relationship occurs between the phases of two synchronized self-sustained oscillators is often termed *phase locking* [1]–[3]. Synchronization is thus often described in terms of phase locking, while in the synchronization state the phase difference is always taken to be bounded.

In order to analyze all possible dynamical behaviors, we use what is called *phase space*, meaning the multi-dimensional euclidean space whose points corresponds to the initial conditions of unique solutions of the equations of motion. We define each system's evolving position in time as forming a *phase space trajectory*, which is the set of all its states consistent with the given initial condition.

In the presence of dissipation, the onset of stable oscillations is mathematically described by the attraction of trajectories to an isolated periodic solution of the system, whose trajectory corresponds to a closed curve in phase space called a *limit cycle* [1]–[3]. The case of a simple pendulum serves as an appropriate example that helps us understand the connection between phase space and time evolution of its trajectories (Figure 3).

When dissipation and driving forces balance, the system settles into its typical behavior, which is called an *attractor*. Attractors are clearly seen in phase space, since phase space provides us with the complete evolution of the system's trajectory. Consequently, following this trajectory, we can establish the behavior of the system after long times.

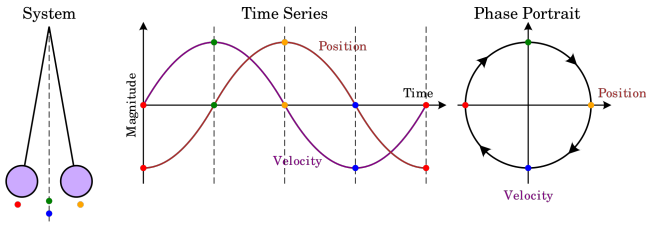

Fig. 3. Phase portrait for the motion of a simple pendulum

In phase space an attractor may be a point, a closed curve, a surface or something more complex. We have mentioned above one of the simplest types of attractors called limit cycle and consisting of a closed curve. However, there exist more complex attractors, called *strange attractors*, on which the dynamics behaves unpredictably and chaotically. In the early 1960s, Lorenz studied a simplified model of convection rolls in the atmosphere above a lake to gain insight into the notorious unpredictability of the weather. In its simplest form, this atmospheric convection model is a system of three ordinary differential equations now known as the Lorenz equations [1]–[3]:

$$\begin{aligned} \dot{x} &= \sigma(y - x) \\ \dot{y} &= x(\rho - z) - y \\ \dot{z} &= xy - \beta z \end{aligned} \tag{3}$$

Typical values values for which this system exhibits chaotic behavior are $\sigma = 10$, $\beta = 8/3$ and $\rho = 28$. Lorenz found that the solutions of his equations (3) never settled down to equilibrium or to a periodic state. Instead, they continued to oscillate in an irregular, aperiodic fashion. He also showed that there was a structure in chaos, as all solutions of his equations, when plotted in three dimensions, evolved onto a butterfly-shaped *fractal* set of points [1]–[3] (Figure 4).

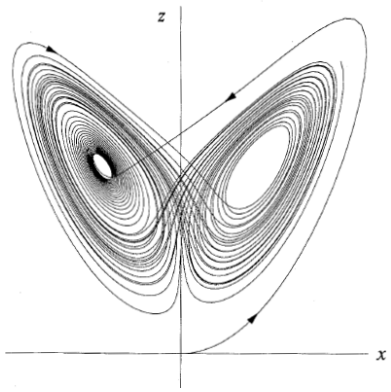

Fig. 4. The strange attractor of the Lorenz equations.

Let us now describe the phenomenon of a *chimera state*, which is a fascinating topic in nonlinear dynamics that has attracted great interest in recent years [4]–[7]. As mentioned earlier, it is the coexistence of synchronous and asynchronous oscillations in the dynamics of large systems of coupled oscillators.

The applications of such fascinating dynamics are numerous and range over a wide variety of networks of nonlinear systems. For example, there is evidence that confirms the relevance of chimera states in real-life phenomena, such as the uni-hemispheric sleep observed in birds and dolphins, where one hemisphere of the brain is synchronous and the other is asynchronous. Systems with chimera states occur not only in mechanics [4], [6], engineering [5] and biology [8], but also in *photonics*, which is a very important field of science that our research focuses on [9], [10].

Photonics has many applications in medicine, optics, space communications etc. In particular, it advances the important field of communications, providing new opportunities to transmit information by light. In fact, one major NASA priority is to use photons to make space communications for both near-Earth and deep-space missions more efficient.

A. The example of the Li-Sprott oscillator

Generally, strange attractors and limit cycles are isolated and occur in most systems by themselves. However, there exist systems of NODEs that possess *coexisting attractors* of different types. One such system, representing a 4–Dimensional (4D) set of simplified Lorenz equations was studied by Li and Sprott [11].

$$\begin{aligned} \dot{x} &= y - x \\ \dot{y} &= -xz + u \\ \dot{z} &= xy - a \\ \dot{u} &= -by \end{aligned} \tag{4}$$

In [12], the authors obtained many interesting results, such as the coexistence of a torus with symmetric pair of limit cycles, the coexistence of a symmetric pair of strange attractors with a limit cycle, etc. Every of them is very interesting and has a deep meaning, regarding the behavior of nonlinear systems in general. In this MSc thesis, we will be concerned only with the choice of parameters $a = 7$ and $b = 0.1$ in (4), for which there is coexistence of a limit cycle with two symmetric strange attractors (see Figure 5).

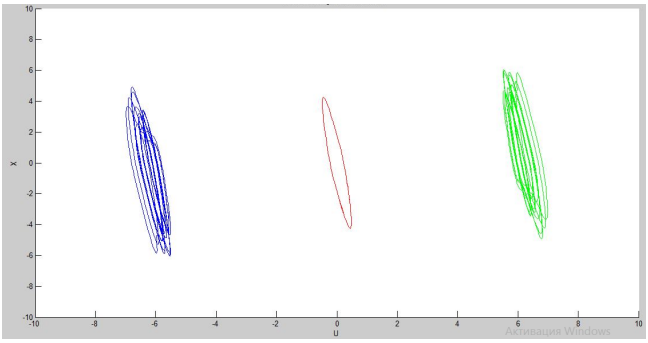

Fig. 5. A limit cycle coexists with a symmetric pair of strange attractors at $a = 7$, $b = 0.1$(green and blue attractors correspond to two symmetric initial conditions $(\pm 14.1, 0, 20, 0)$ and red at initial conditions $(-1, 0, -1, 0)$)

In Section II we will investigate in detail the above oscillator and extend the results described in [12] to study networks of such oscillators, focusing in particular on the existence of synchronous as well as asynchronous oscillations that generate the fascinating phenomenon of chimera states.

B. Nonlinear Laser Dynamics

Coupled semiconductor lasers are systems possessing complex dynamics that are interesting for numerous applications in photonics [13]–[17]. First of all, we will investigate here the dynamics of a single photonic dimer, which consists of two evanescently coupled lasers $(M = 2)$. The dynamics of an array of such a laser dimer is governed by the following equations describing the slowly varying complex amplitude of the normalized electric fields $\epsilon_i, i = 1, 2$ and the normalized excess carrier density $N_i, i = 1, 2$ of each laser [18]–[20]:

$$\begin{aligned} \tfrac{d\epsilon_1}{dt} &= (1 - i\alpha)\epsilon_1 N_1 + i\eta\epsilon_2 + i\omega_1\epsilon_1 \\ T\tfrac{dN_1}{dt} &= P_1 - N_1 - (1 + 2N_1)|\epsilon_1|^2 \\ \tfrac{d\epsilon_2}{dt} &= (1 - i\alpha)\epsilon_2 N_2 + i\eta\epsilon_1 + i\omega_2\epsilon_2 \\ T\tfrac{dN_1}{dt} &= P_2 - N_2 - (1 + 2N_2)|\epsilon_2|^2 \end{aligned} \tag{5}$$

where α is the linewidth enhancement factor, η is the normalized coupling constant, P is the normalized excess electrical pumping rate, ω is the normalized optical frequency detuning from a common reference, T is the ratio of carrier to photon lifetimes, and t is the normalized time.

The properties of such a pair of coupled lasers are determined mostly by its stationary states and their stability, which can be controlled by the current injection in the two lasers. Coupled laser

behavior has been investigated in terms of a model including both laser coupling and carrier density dynamics. The crucial role of carrier density dynamics has been taken into account by considering a model where the field equations are dynamically coupled with the carrier density equations.

Detuning and pumping between the lasers plays a remarkable role in the dynamics of coupled lasers. When the detuning is zero, there exist stable *asymmetric* modes despite the homogeneous pumping between the lasers. The lasers are absolutely symmetric. However, in the case of nonzero detuning, there exist *phase-locked* (i.e.limit cycle) modes with arbitrary power, amplitude ratio and phase difference for appropriate selection of pumping and detuning values.

Thus, remarkably, arbitrary asymmetry can be achieved by appropriate selection of the detuning and the pumping of the system. The existence of stable asymmetric phase-locked states with unequal field amplitudes and phase differences for the pair of coupled lasers crucially determines its far field patterns and the capabilities of such a system as building block for synthesizing larger controllable active structures characterized by complex dynamics [21]. The asymmetry relates to operation conditions that result in the presence of gain in one laser and loss in other. The role of the current injection suggests a dynamic mechanism for the control of the phase-locked states and, therefore, the far-field emission patterns of this fundamental photonic element, consisting of two coupled lasers.

As preliminary results, we aimed to understand more deeply the case of two coupled lasers $(M = 2)$, and solved numerically the equations of motion (5) and obtained limit cycles for certain parameter values of field amplitude ratio ρ and phase difference θ shown in Figure 6. In the particular case $\rho = 0.5$, the phase-locked states become unstable and the system evolves to a stable limit cycle shown in Figure 6. Thus, in this figure we see that laser oscillators possess stable limit cycles, while for others chaotic states are possible [18], [19].

Based on these results for a single dimer, after establishing and determining some parameter regions for which limit cycles and chaotic behavior occur, we turned to the study of an array (or network) of $M > 2$ coupled lasers to investigate whether synchronization occurs there also. Our aim was to avoid the occurrence of chaos, as well as chimera states, which after all constitute a partial loss of synchronization.

The results for a single dimer motivated us to investigate the dynamics of coupled laser oscillators in more detail. In particular, we are interested in a study of synchronization phenomena in *laser arrays* as a basic tool creating a source of high-intensity radiation. This can be achieved by coupling the lasers in a linear network so that they interact only with their nearest neighbors. The case of interactions with *groups* of neighbor elements, in the form of global coupling [22], is the result of an ongoing investigation, which is more difficult, but very worthwhile, since it may turn out to be experimentally realistic in laser arrays.

In closing this Section, we would like to mention is another very interesting phenomenon that arises in networks of coupled nonlinear oscillators called *Kuramoto self-synchronization transition.* [4]. It is applicable when nonidentical phase oscillators with different frequencies are coupled. When two oscillators have very close frequencies they easily synchronize. As a result, their contribution to the mean field at the frequency of these synchronous oscillations increases. This increased component of the driving force naturally entrains other elements that have close frequencies and this leads to the growth of synchronized clusters and to a further increase of the component of the mean field at a certain frequency [4]. So, based on these observations and information, we plan to extend our goals in the future and also investigate the occurrence of Kuramoto self-synchronization in photonic arrays.

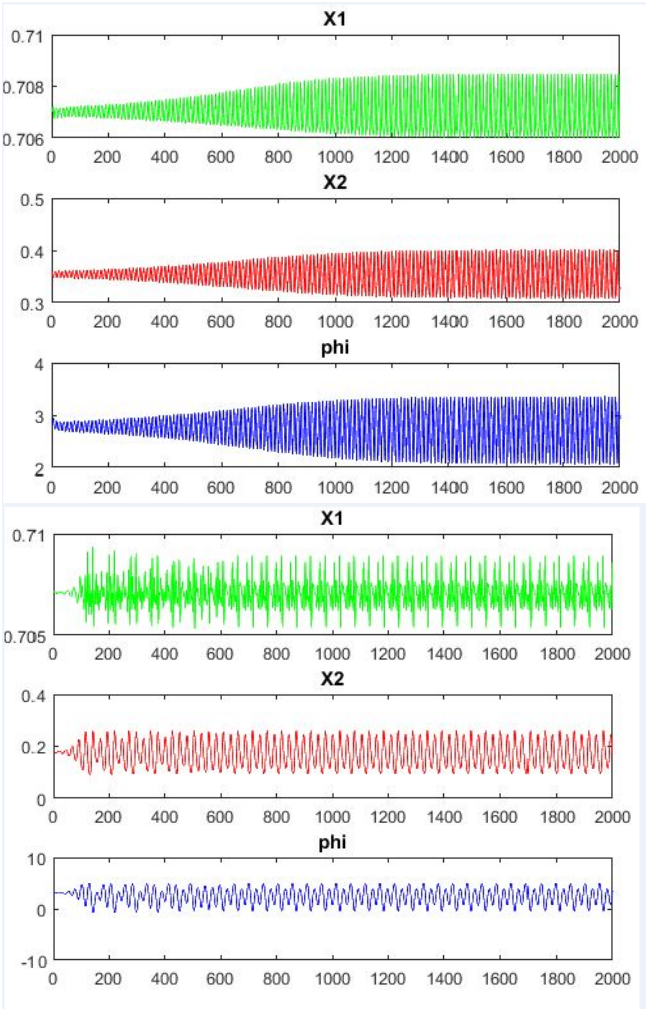

Fig. 6. Time evolution of the electric field amplitude and phase difference. Initial conditions correspond to asymmetric phase-locked states with $\theta = 0.9\pi$ an d $\rho = 0.5, 0.25$

II. System of coupled Li-Sprott oscillators

We start our study of oscillatory phenomena by considering the behavior of a single Li-Sprott oscillator of the form (4) comprehensively, after which we will proceed to examine more carefully the network's dynamics. The results previously obtained for oscillators of the above type motivated us to determine whether the behavior of a single oscillator can influence the dynamics of the whole system. Such analysis, regarding the influence of single oscillator's behavior to dynamics of whole system was studied in [12]. As we mentioned above, in this section we will investigate in detail the above oscillator and extend the results described in [12] to study networks of such oscillators, focusing in particular on the existence of synchronous as well as asynchronous oscillations that generate the fascinating phenomenon of chimera states. Thus we focused on a network of non-locally coupled such systems, as described in detail in [12]. Every single unit of this network is described by a single Li-Sprott(L-S) oscillator of the form (4) [11]. To construct our network, we will couple $N = 100$ such L-S oscillators on a one-dimensional ring. The coupling is non-local, and we use connections in such a way that each network element is coupled to its $2P$ nearest neighbors (see Figure 7) [12]. The equations of the coupled oscillators are given as follows:

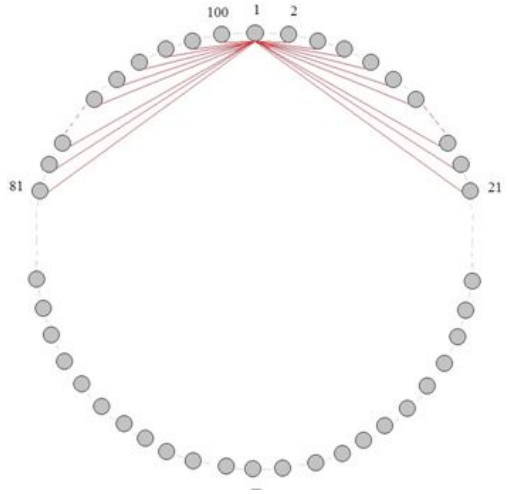

Fig. 7. Representation of the coupled oscillators (2) on a ring. Each oscillator interacts with P = 20 neighbors on its left and 20 on its right.

$$\begin{aligned} \dot{x_i} &= y_i - x_i + \tfrac{d}{2P}\textstyle\sum_{j=(i-P)modN}^{(i+P)modN}[x_j - x_i],\ \ 1 \leq kmodN \leq N \\ \dot{y_i} &= -x_i z_i + u_i \\ \dot{z_i} &= x_i y_i - a \\ \dot{u_i} &= -b y_i \end{aligned} \tag{6}$$

where $i = 1, 2....N$ and d is the coupling strength and the $modN$ notation implies that we coupled together every $1 \leq j \leq N$, oscillators, with $P = 20$.

A. Analytical approximation of limit cycles

The limit cycles of the Li-Sprott system (II) are clearly very important for the formation of large synchronized clusters. It is, therefore, interesting to approximate analytically the basic properties of limit cycles in such models. Such analysis, regarding the derivation of formulas for the frequency and amplitude of limit cycles for a single L-S oscillator, was succesfully performed in [12]. We have thus decided in this thesis to extend thia analysis to the case of many coupled L-S oscillators to derive approximate but analytic formulas for their limit cycle oscillations.

We present this analysis below for a system of NODEs describing an $(N = 3)$ 3-particle ring of Li-Sprott oscillators, and omit the generalization to arbitrary N, since it is a straightforward

extension of the results presented below. Let us begin with the system of equations obtained from (II) for $N = 3$:

$$\begin{aligned} \dot{x_i} &= y_i - x_i + \tfrac{d}{2}(x_{i+1} - x_i + x_{i+2} - x_i) \\ \dot{y_i} &= -x_i z_i + u_i, \qquad i = 1, 2, 3 \\ \dot{z_i} &= x_i y_i - a \\ \dot{u_i} &= -b y_i, \end{aligned} \tag{7}$$

cyclically, i.e. $x_i = x_{i+3}$. We wish to approximate the limit cycle motion of all 3 oscillators, assuming that they have all reached a synchronized state, where all their frequencies are equal to a single ω. All oscillators are taken to execute periodic motion around the origin of the 12-D phase space, albeit each each with possibly different amplitudes and phases. Thus, following [12], the trial solutions we use to find periodic solutions of limit cycle type are of the form:

$$\begin{aligned} x_i &= A_i \cos(\omega t) + B_i \sin(\omega t) \\ y_i &= C_i \cos(\omega t) + D_i \sin(\omega t) \\ z_i &= E_i \cos(2\omega t) + F_i \sin(2\omega t) \\ u_i &= G_i \cos(\omega t) + H_i \sin(\omega t) \end{aligned} \tag{8}$$

The case of z_i having twice the frequency of the other variables is used because it was shown to be necessary in the analysis of the single-oscillator case [12], where the obtained results were found to reproduce the numerical values of the frequency to and amplitude of all variables to satisfactory accuracy.

Thus, substituting (8) in (7), we find from eq. (7a):

$$\begin{aligned} -\omega A_1 \sin \omega t + \omega B_1 \cos wt = (C_1 - A_1) \cos wt + (D_1 - B_1) \sin \omega t + \frac{d}{2}[(A_2 - A_1) \cos \omega t + \\ + (B_2 - B_1) \sin \omega t + (A_3 - A_1) \cos \omega t + (B_3 - B_1) \sin \omega t] \end{aligned} \tag{9}$$

for $i = 1$ and two more similar equations for $i = 2, 3$. Equating in these equations the coefficients of $cos(\omega t)$ and $sin(\omega t)$, we obtain the following algebraic system involving the unknown frequency and amplitudes of the oscillators:

$$\begin{aligned} -\omega A_1 &= D_1 - B_1 + \frac{d}{2}[B_2 + B_3 - 2B_1] \\ -\omega B_1 &= C_1 - A_1 + \frac{d}{2}[A_2 + A_3 - 2A_1] \\ -\omega A_2 &= D_2 - B_2 + \frac{d}{2}[B_3 + B_1 - 2B_2] \\ -\omega B_2 &= C_2 - A_2 + \frac{d}{2}[A_3 + A_1 - 2A_2] \\ -\omega A_3 &= D_3 - B_3 + \frac{d}{2}[B_2 + B_1 - 2B_3] \\ -\omega B_3 &= C_3 - A_3 + \frac{d}{2}[A_2 + A_1 - 2A_3] \end{aligned} \tag{10}$$

Similarly, substituting from eq. (8) into eq.(7b) we have :

$$\begin{aligned} -\omega C_i \sin \omega t + \omega D_i \cos \omega t = -(A_i E_i \cos \omega t \cos 2\omega t + B_i F_i \sin \omega t \sin 2\omega t + \\ + E_i B_i \sin \omega t \cos 2\omega t + A_i F_i \cos \omega t \sin 2\omega t) + G_i \cos \omega t + H_i \sin \omega t \end{aligned} \tag{11}$$

Noting now that:

$$\begin{aligned}\cos\omega t\cos 2\omega t &= \frac{1}{2}(\cos 3\omega t + \cos\omega t)\\ \sin\omega t\sin 2\omega t &= \frac{1}{2}(-\cos 3\omega t + \cos\omega t)\\ \sin\omega t\cos 2\omega t &= \frac{1}{2}(\sin 3\omega t - \sin\omega t)\\ \cos\omega t\sin 2\omega t &= \frac{1}{2}(\sin 3\omega t + \sin\omega t)\end{aligned} \tag{12}$$

we find that eq. (11) yields, dropping the $\cos 3\omega t$, $\sin 3\omega t$ terms, the following equations, upon equating terms proportional to $cos(\omega t)$ and $sin(\omega t)$:

$$\begin{aligned}-\omega C_i &= \frac{1}{2}E_iB_i - \frac{1}{2}A_iF_i + H_i\\ -\omega D_i &= -\frac{1}{2}E_iA_i - \frac{1}{2}B_iF_i + H_i\end{aligned} \tag{13}$$

where $i = 1, 2, 3$. Similarly, from eq. (7c) we obtain:

$$\begin{aligned}-2\omega E_i\sin 2\omega t + 2\omega F_i\cos 2\omega t = (A_iC_i(\cos\omega t)^2 + B_iD_i(\sin\omega t)^2\\ +(C_iB_i + A_iD_i)\sin\omega t\cos\omega t) - a\end{aligned} \tag{14}$$

Expressing now the quantities $cos^2(\omega t)$ and $sin^(\omega t)$ in terms of $cos(2\omega t)$ and $sin(2\omega t)$ and equating the corresponding terms we arrive at the equations:

$$\begin{aligned}-2\omega E_i &= (B_iC_i + A_iD_i)\frac{1}{2}\\ 2\omega F_i &= (A_iC_i - B_iD_i)\frac{1}{2}\\ 2a &= A_iC_i + B_iD_i\end{aligned} \tag{15}$$

Finally, proceeding in the same way, we obtain from eq. (7d):

$$\omega G_i = bD_i, \quad \omega H_i = -bC_i, \;\; i = 1, 2, 3 \tag{16}$$

Using (16) we now rewrite (13) in the form:

$$\begin{aligned}(\frac{b}{\omega} - \omega)C_i &= \frac{1}{2}E_iB_i - \frac{1}{2}A_iF_i\\ (-\frac{b}{\omega} + \omega)D_i &= -\frac{1}{2}E_iA_i - \frac{1}{2}B_iF_i\end{aligned} \tag{17}$$

Let us solve system (17) for E_i, F_i:

$$\begin{aligned}E_i &= \frac{2(\frac{b}{\omega} - \omega)(C_iB_i + D_iA_i)}{(B_i)^2 + (A_i)^2}\\ F_i &= \frac{2(\frac{b}{\omega} - \omega)(D_iB_i - C_iA_i)}{(B_i)^2 + (A_i)^2}\end{aligned} \tag{18}$$

Comparing equations (18) and (15) and solving for $E_i \neq 0$ and $F_i \neq 0$, we obtain the following equations correspondingly:

$$\begin{aligned}(A_i)^2 + (B_i)^2 &= 8(\omega^2 - b)\\ 4\omega &= ((A_i)^2 + (B_i)^2)/2(-\frac{b}{\omega} + \omega)\end{aligned} \tag{19}$$

where $i = 1, 2, 3$.
In view of (19), equations (18) give:

$$\begin{aligned} E_i &= \frac{2(\frac{b}{\omega} - \omega)(C_i B_i + D_i A_i)}{8(\omega^2 - b)} = \frac{-1}{4\omega}(C_i B_i + D_i A_i) \\ F_i &= \frac{2(\frac{b}{\omega} - \omega)(D_i B_i - C_i A_i)}{8(\omega^2 - b)} = \frac{-1}{4\omega}(D_i B_i - C_i A_i) \end{aligned} \tag{20}$$

which, of course, are the same as equations (15).

Now we have 6 equations from (10) and 3 equations from (19), including also (15c), for the 12 unknown amplitudes A_i, B_i, C_i, D_i, $i = 1, 2, 3$ and the unknown frequency ω. Observe that once these equations are solved the variables E_i, F_i are directly obtained from eq. (18).

Note that from (19) we obtain the following equations:

$$(A_i)^2 + (B_i)^2 = 8(\omega^2 - b) \tag{21}$$

and also

$$4(\omega^2 - b) = \frac{2a}{1 + \frac{3d}{2}} \tag{22}$$

from which it follows that

$$\omega^2 = \frac{a}{4 + 6d} + b \tag{23}$$

which agrees with the result for $d = 0$ [12].

So, in the fully coupled case, we have thus obtained an expression for the frequency of oscillations of the system, when all limit cycles are synchronized:

$$\omega^2 = \frac{a}{4 + 6d} + b \tag{24}$$

After obtaining a formula for the frequency, let us now try to derive an approximation for the amplitudes of oscillation. To this end, we will substitute in eq. (10) :

$$A_i = \alpha_i \sin\psi_i, \quad B_i = \alpha_i \cos\psi_i, \quad C_i = \beta_i \sin\eta_i, \quad D_i = \beta_i \cos\eta_i, \ \imath = 1, 2, 3. \tag{25}$$

writing our oscillation variables in the form

$$x_i = \alpha_i \sin(\omega t + \psi_i), \quad y_i = \beta_i \sin(\omega t + \eta_i), \quad z_i = \gamma_i \sin(2\omega t + \theta_i), \quad u_i = \delta_i \sin(\omega t + \zeta_i) i = 1, 2, 3. \tag{26}$$

Using these formulas to substitute in (19), we find:

$$\alpha_i^2 = \frac{2a}{1 - \frac{d}{2}}, \quad \alpha_i = \alpha = 8(\omega^2 - b) \tag{27}$$

Let us now go to equations (15)(c) and rewrite them as follows:

$$\alpha_1\beta_1 \cos(\psi_1 - \eta_1) = 2a, \quad \alpha_2\beta_2 \cos(\psi_2 - \eta_2) = 2a, \quad \alpha_3\beta_3 \cos(\psi_3 - \eta_3) = 2a \tag{28}$$

All these equations now reduce to

$$\beta_i = \frac{2a}{\alpha_i \cos(\psi_i - \eta_i)} = \frac{2a}{\alpha \cos(\psi_i - \eta_i)} \tag{29}$$

Using the above formulation we may rewrite equations (10) in the following form:

$$\begin{aligned}
-\omega \sin\psi_1 &= \frac{\beta_1}{\alpha}\cos\eta_1 - (1+\frac{d}{2})\cos\psi_1 + \frac{d}{2}(\cos\psi_2 + \cos\psi_3)\\
\omega \cos\psi_1 &= \frac{\beta_1}{\alpha}\sin\eta_1 - (1+\frac{d}{2})\sin\psi_1 + \frac{d}{2}(\sin\psi_2 + \sin\psi_3)\\
-\omega \sin\psi_2 &= \frac{\beta_2}{\alpha}\cos\eta_2 - (1+\frac{d}{2})\cos\psi_2 + \frac{d}{2}(\cos\psi_3 + \cos\psi_1)\\
\omega \cos\psi_2 &= \frac{\beta_2}{\alpha}\sin\eta_2 - (1+\frac{d}{2})\sin\psi_2 + \frac{d}{2}(\sin\psi_3 + \sin\psi_1)\\
-\omega \sin\psi_3 &= \frac{\beta_3}{\alpha}\cos\eta_3 - (1+\frac{d}{2})\cos\psi_2 + \frac{d}{2}(\cos\psi_1 + \cos\psi_2)\\
\omega \cos\psi_3 &= \frac{\beta_3}{\alpha}\sin\eta_3 - (1+\frac{d}{2})\sin\psi_3 + \frac{d}{2}(\sin\psi_1 + \sin\psi_2)
\end{aligned} \tag{30}$$

and since we are seeking synchronized behavior, where variables oscillate in phases in phase, we shall consider all η_i, and all ψ_i equal respectively, i.e. $\psi \equiv \psi_1 = \psi_2 = \psi_3$, and $\eta \equiv \eta_1 = \eta_2 = \eta_3$. This leads us to

$$\beta_i = \beta = \frac{2a}{\alpha\cos(\psi - \eta)} \tag{31}$$

Thus, all of the equations (30) above, reduce to a single one (31), which expresses the amplitude of the y variables as a function of the amplitude of the x variables and their phase difference.

Summarizing, we now have obtained expressions for the frequency of limit cycle oscillations

$$\omega^2 = \frac{a}{4+6d} + b \tag{32}$$

as well as the amplitudes of the oscillations in (x, y) space,

$$\alpha^2 = \frac{2a}{1-\frac{d}{2}}, \quad \beta_i = \beta = \frac{2a}{\alpha\cos(\psi-\eta)} \tag{33}$$

from which the amplitudes of the z and u variables can also be obtained through eq. (20) and (16).

B. Synchronization and chimera states in networks of L-S oscillators

Basins of attractions for the limit cycle and two strange attractors of system (4) with $a = 7$ and $b = 0.1$, which is the case we study in this MSc thesis, was obtained in [12]. About the origin it is very large for the limit cycle compared to those of the two strange attractors on its right and left side, see Fig. (8) [12]. Basins of attraction play a very important role in the findings of the coupled system (6).

Of course, the coupling strength also plays a very important role in the system's global coherence and synchronization properties. When there is no coupling, the network is completely incoherent, while by increasing the coupling, full synchronization, as well as different types of chimera states begin to emerge. As the coupling grows, a fascinating kind of partial synchronization occurs which leads to true chimera states with one head, two heads and 4 heads [12].

In order to understand the dynamics of the system (6) more deeply, we first repeated all the calculations performed in [12]. Using MATLAB we recovered not only the coexistence of limit cycle and two strange attractors, but also some of the chimera states (see Figure 9). As we see, increasing coupling strength (d), for random initial conditions, correspondingly we obtain *perfect chimera states* with increasing number of heads. There heads of Chimera is created by asynchronous oscillators, while other are synchronous.

Taking also into consideration certain initial conditions from the basin of attraction of the limit cycles, we can obtain *imperfect chimera states*, where most particles are started from the basin attraction of the limit cycle and oscillate coherently, while a number of "rebels", whose initial conditions are chosen close to the vicinity of the strange attractors, escape and begin to oscillate differently from all others (see Figure 10).

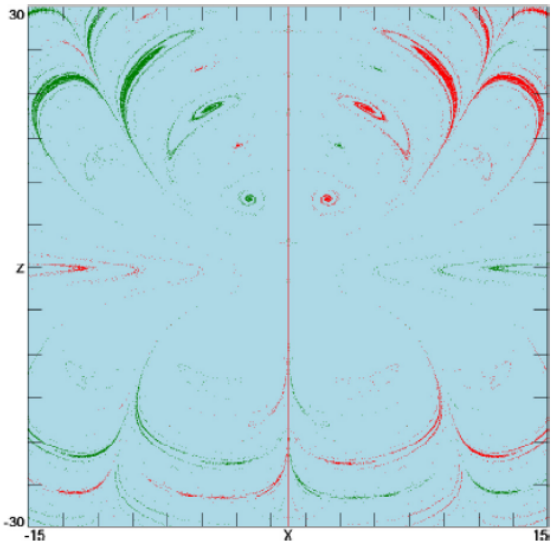

Fig. 8. Basin of attraction of initial conditions leading to the central limit cycle (blue) and those leading to the two strange attractors (red).

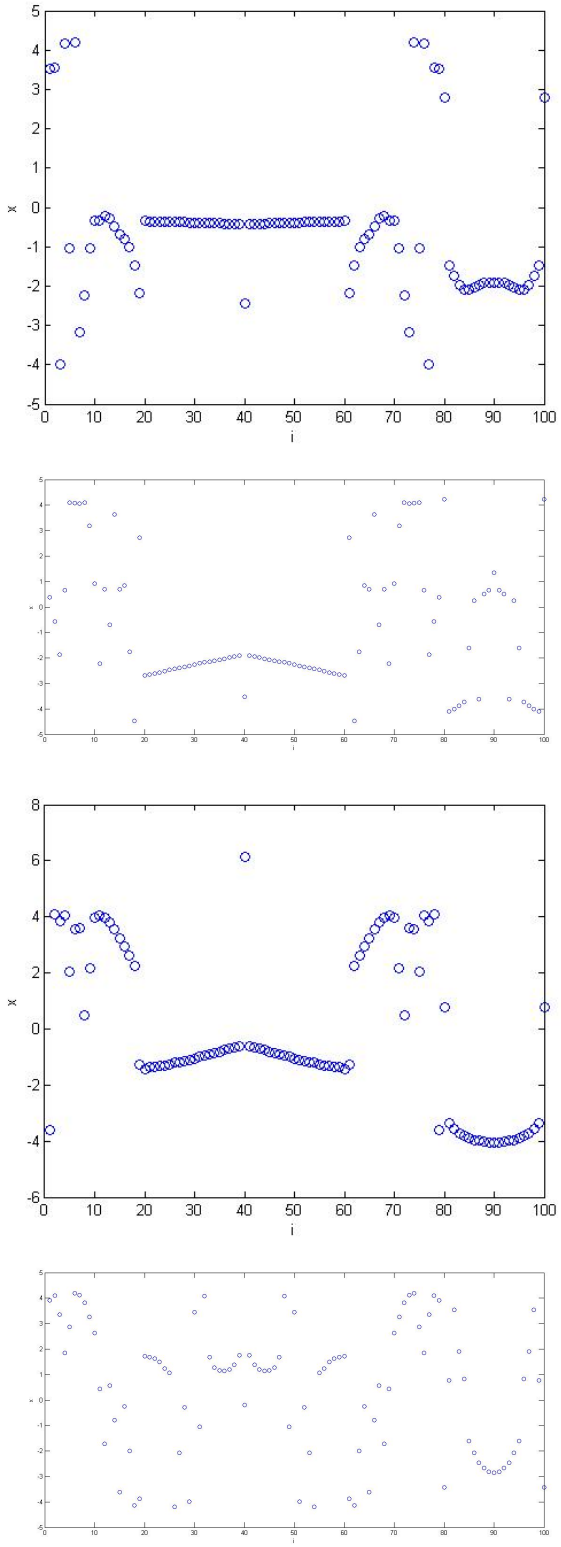

Fig. 9. All initial conditions are zero, coupling parameter is correspondingly $d = 0.002, 0.005, 0.007, 0.009$

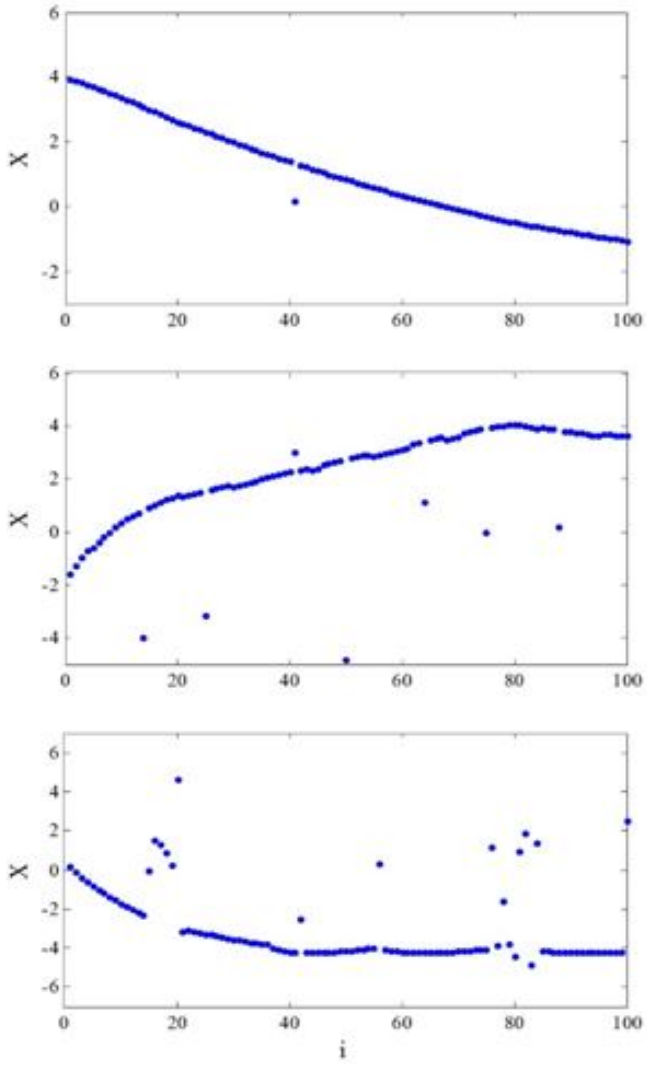

Fig. 10. Snapshots of spatiotemporal patternsof system, imperfect synchronization for corresponding coupling parameters d=0.005, d=0.005 but for different initial conditions, d=0.01

III. OSCILLATORY PHENOMENA IN ARRAYS OF LASER DIMERS

A. Synchronization in a single laser dimer

Before studying arrays of laser dimers, we have worked on the dynamics of a single dimer, consisting of two lasers. The existence and stability of phase-locked states for a pair of coupled lasers of this type, under symmeric and asymmetric electrical pumping, were investigated in [9]. Using rescaled and rewritten forms of (5) from [9], we proceed to find fixed points (equilibria) of the dynamical system Eq(5). The frequency was defined using a reference value of pumping P:

$$\Omega = \sqrt{\frac{2P}{T}} \tag{34}$$

Using this expression for a single dimer (5) was rescaled in [9] as

$$\begin{array}{l} \frac{d\epsilon_1}{d\tau} = (1 - i\alpha)\epsilon_1 N_1 + i\Lambda\epsilon_2 + i\Omega_1\epsilon_1 \\ 2P\frac{dN_1}{d\tau} = P_1 - \Omega N_1 - (1 + 2\Omega N_1)|\epsilon_1|^2 \\ \frac{d\epsilon_2}{d\tau} = (1 - i\alpha)\epsilon_2 N_2 + i\Lambda\epsilon_1 + i\Omega_2\epsilon_2 \\ 2P\frac{dN_2}{d\tau} = P_2 - \Omega N_2 - (1 + 2\Omega N_2)|\epsilon_2|^2 \end{array} \tag{35}$$

where
$\tau \equiv \Omega t$, $N_i \equiv \frac{N_i}{\Omega}$, $\Lambda \equiv \frac{\eta}{\Omega}$, $\Omega_i \equiv \frac{\omega_i}{\Omega}$.

By introducing the amplitude and phase in the complex electric fields of the lasers as $\epsilon_i = X_i \exp i\theta_i$, equations (35) become as:

$$\begin{array}{l} \frac{dX_1}{d\tau} = X_1 N_1 - \Lambda X_2 \sin\theta, \\ \frac{dX_2}{d\tau} = X_2 N_2 + \Lambda X_2 \sin\theta, \\ \frac{d\theta}{d\tau} = \Delta - \alpha(N_2 - N_1) + \Lambda(\frac{X_1}{X_2} - \frac{X_2}{X_1})\cos\theta \\ 2P\frac{dN_1}{d\tau} = P_1 - \Omega N_1 - (1 + 2\Omega N_1)X_1^2, \\ 2P\frac{dN_2}{d\tau} = P_2 - \Omega N_2 - (1 + 2\Omega N_2)X_2^2. \end{array} \tag{36}$$

Thus, we will work on these last equations. The equilibria of the dynamical system of Eq. (36) are given as the solutions of the algebraic system obtained by setting the time derivatives of the system equal to zero and their linear stability is determined by the eigenvalues of the Jacobian of the system.

For the case of zero detuning ($\Delta = 0$) and symmetric electrical pumping ($P_1 = P_2 = P_0$) equilibria states are displayed analytically in [9], [18], [19]. This case is defined as "oscillation death" scenario in [9].

Since our purpose is to study synchronous properties of coupled oscillators, we are mainly interested in periodic solutions of the system. So, we consider the case of nonzero detuning ($\Delta \neq 0$). Since analytic solutions of the system of equations that provide the field amplitudes and phase difference for a given set of laser parameters can not be obtained, the reverse problem was solved explicitly in [9]: for a given phase locked state with field amplitude ratio $\rho \equiv \frac{X_2}{X_1}$ and phase difference θ, the algebraic system of equations obtained by setting the right-hand side of (36) equal to zero are solved to determine the steady-state carrier densities $N_{1,2}$ as well as the appropriate detuning (Δ) and pumping rate (P) in terms of *field amplitude ratio* $\rho = \frac{X2}{X1}$ and *phase difference* θ. So,we obtain:

$$\begin{array}{l} N_1 = \Lambda\rho\sin\theta, \\ N_2 = -\frac{\Lambda}{\rho}\sin\theta, \\ \Delta = -\alpha\Lambda\sin\theta(\frac{1}{\rho} + \rho) - \Lambda\cos\theta(\frac{1}{\rho} - \rho), \\ P_1 = X_0^2 + (1 + 2X_0^2)\Omega\Lambda\rho\sin\theta, \\ P_2 = \rho^2 X_0^2 - (1 + 2\rho^2 X_0^2)\frac{\Omega\Lambda}{\rho}\sin\theta. \end{array} \tag{37}$$

Therefore, there always exists a phase-locked state with arbitrary field amplitude asymmetry and phase difference, provided that the detuning and pumping rates values are given, as in (37). These

phase-locked states exist in the whole parameter space and can have arbitrary power X_0. However, their stability strongly depends on the coupling Λ as well as the power (X_0) and the degree of their asymmetry, characterized by ρ and θ. Typical configurations relevant to experiments as $P = 0.5$, $\alpha = 5$ and $T = 500$ were used in [9].

So, using the above parameters, putting $\theta = 0.9\pi$ and choosing $\Lambda = 10^{-2.1}$ from stability regions of phase-locked states of arbitrary asymmetry, characterized by the ρ and θ [9], we solved equations (5) and obtained numerically stable limit cycles for certain parameter values of field amplitude ratio ρ and phase difference θ shown in Figure 6. In the particular case $\rho = 0.5$, the phase-locked states become unstable and the system evolves to a stable limit cycle shown in Figure 6.

B. Large and small amplitude oscillations in laser dimer arrays

Motivated by studies on a single dimer, we are now interested in the collective behavior of a large array of semiconductor lasers with nearest-neighbor interactions [22]. The crucial parameters for the observed dynamics are the pumping rates and the relative optical frequency detuning between the lasers, both of which introduce realistic inhomogeneities and dispersions within our coupled pairs of semiconductor lasers. We find that localized oscillations close to the fixed point coexist with large amplitude oscillations where their field amplitudes and phases can be dynamically controlled by appropriate gain values in each dimer. This investigation has been done from a fundamental level of a dimer up to a large array of 100 dimers. In both levels, it has been shown that the coexistence of localized oscillations close to the fixed point (LOCFP) and large amplitude oscillations (LAO) is possible even in the presence of random frequency detuning between the coupled lasers. The coupling strength has been proved to be sufficient to generate this type of dynamics for a pair of coupled lasers, without significantly disturbing the next coupled neighbour dimer, allowing thus for a full space control by combining different clusters inside the array with LOCFP or LAO properties.

The dynamics of our laser array for the slowly varying complex amplitudes ε_j of the electric fields inside the lasers and for the corresponding population inversions N_j, is described by the following rate equations [22]:

$$\frac{d\varepsilon_j^A}{dt} = (1 - i\alpha)N_j^A\varepsilon_j^A + i\eta(\varepsilon_{j+1}^B + \varepsilon_{j-1}^B) + i\omega_j^A\varepsilon_j^A \tag{38a}$$

$$\frac{d\varepsilon_j^B}{dt} = (1 - i\alpha)N_j^B\varepsilon_j^B + i\eta(\varepsilon_{j+1}^A + \varepsilon_{j-1}^A) + i\omega_j^B\varepsilon_j^B \tag{38b}$$

$$T\frac{dN_j^A}{dt} = P_j^A - N_j^A - (1 + 2N_j^A)|\varepsilon_j^A|^2 \tag{38c}$$

$$T\frac{dN_j^B}{dt} = P_j^B - N_j^B - (1 + 2N_j^B)|\varepsilon_j^B|^2\,. \tag{38d}$$

where $1 \leq j \leq M$, with $M = 200$ the number of lasers. The dimensionless time t and the population inversion decay time T are measured in units of the field decay time. The amplitude-phase coupling is modeled by the linewidth enhancement factor $\alpha = 5$. P_j are the pump coefficients and η is the normalized coupling rate between neighboring lasers. The normalized angular frequency ω_j measures the detuning of laser j from a common reference. The superscripts A and B denote the electric field in two different sublattices.

C. Oscillations in one laser dimer

Having defined the equations of the system, we proceed by first considering two coupled lasers each one with a proper pumping rate. The mutual interaction lies on the overlap integrals of both lasers fields [14]. For equal pumping rates and in the absence of detuning the fixed point of the dimer is stable under the condition [23]:

$$\eta < \frac{1 + 2P}{2aT} \tag{39}$$

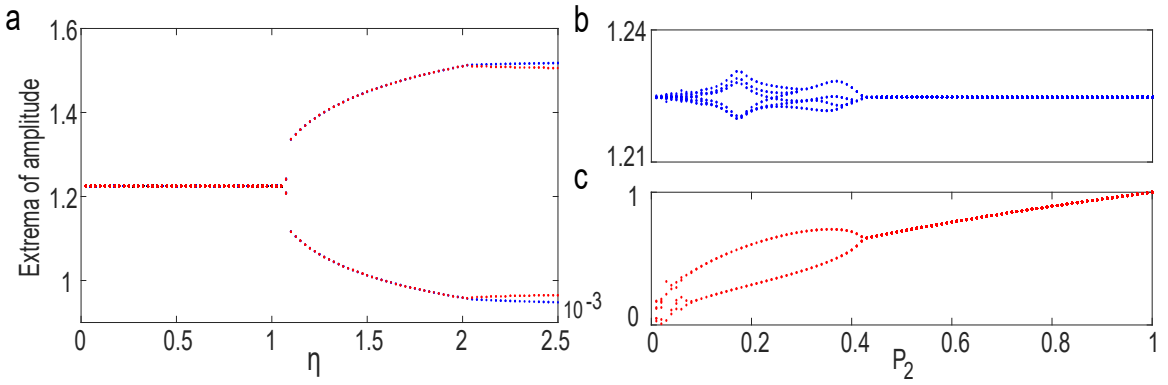

Fig. 11. (a) Extrema of the amplitude of the electric field as a function of the coupling streangth η. (a) The blue color refers to the first laser and the red to the second. The steady state undergoes a Hopf bifurcation at $\eta = 0.001$ where $P_1 = P_2 = 1.5$ refer to a dimer of indetical lasers. After the bifurcation point, we observe different extrema of amplitudes for each one of the lasers, even for equal coupling streangth. The right part of the figure shows the extrema of the amplitude of the electric field as a function of the second laser pumping rate. The label (b) refers to the first laser and (c) to the second one. The steady state, undergoes a Hopf bifurcation at $P_2 = 0.42$ with $P_1 = 1.5$ constant. This is the asymmetric case with $\eta = 0.0005$ which corresponds to the fixed point of a dimer with identical lasers. The asymmetry on pumping rates drives the system to the instability where localized oscillations close to the fixed point (first laser (a)) coexist with large amplitude oscillations (second laser (b)). The other parameters are: $a = 5$, $T = 400$ and $\omega_j = 0$.

The diode lasers are pumped electrically with the excess pumping rate $P = 1.5$. By introducing the amplitude and phase of the complex electric field in each laser as $\varepsilon_j = E_j e^{i\theta_j}$ we can calculate each individual variable in the real space.

In order to understand the effect of the coupling strength, Fig.11 (a) depicts a numerically obtained bifurcation diagram of the maxima and minima of the amplitude of the oscillating electric field where each laser has been driven with equal pump ratio. A Hopf bifurcation occurs at $\eta = 0.0013$. As the coupling is increased the limit cycle is born and a period-doubling cascade takes place with different amplitudes for each individual laser. Thus,, by holding the coupling strength at the steady state region ($\eta = 0.0005$), we calculate a bifurcation diagram with P_2 as a parameter and $P_1 = 1.5$ constant, Fig.11 (right column). The steady state then, undergoes a Hopf bifurcation at $P_2 = 0.735$. The frequency of the limit cycle at the Hopf point for this particular system has been numerically calculated for different parameter regions in [9].

A very interesting observation is the large amplitude oscillation of the second laser, in comparison to the first one, Fig.11 (right column). For asymmetric pumping and with $\eta = 0.0005$ corresponding to the fixed point of a dimer with identical lasers the system moves to the instability where localized oscillations close to the fixed point (LOCFP) (Fig.11 (b)) coexist with large amplitude oscillations (LAO) (Fig.11 (c)). This behavior is absent in the previous case of equal pumping and will be crucial when we move to a large array of coupled dimers.

D. Large and small amplitude oscillations in $M > 1$ laser dimers

First of all, we separate our $M-$ dimer array in two different sublattices labeled by A and B which refer to the type of pumping rates applied. With this notation, the array is divided into two clusters where, in the A sublattice the lasers are pumped electrically with the rates $P_j^A = 1$ for $j \in [1, M/2]$ and $P_j^A = 1.5$ for $j \in [M/2+1, M]$ while for the B sublattice, $P_j^B = 1.5$ for $j \in [1, M/2]$ and $P_j^A = 0.7$ for $j \in [M/2+1, M]$, see Fig.12 I. Note that under zero coupling, each second laser of the array belongs to the A sublattice and supports LAO while the others demonstrate LOCFP as mentioned in the previous section.

By turning on the coupling between the dimers ($\eta = 0.0005$) we observe the coexistence of LAO clusters with LOCFP, in Fig.13 (left column). In this figure, we plot the amplitudes of the electric fields for the L (left) and R (right) groups of lasers after $t = 200.000$ time units for both the A sublattice (red dots) and the B sublattice (blue dots) in Fig.13 (b) and (c)). The coupling strength is sufficient for LAO in each individual dimer but not strong enough to transmit this behavior into

the cluster supporting LOCFP. Note that these figures show a "chimera–like" behavior, where the left cluster (L) shows a kind of unsynchronized behavior in relation to the right cluster (R).

Furthermore, Fig.13 (e) and (f) show the case where only the 50th laser's pumping rates are different than the rest. A graphical sketch of this network was shown in Fig.12 II. Note that here we observe a "breather–like" behavior where only the middle laser is oscillating, while all others are practically at rest. Our initial conditions throughout the manuscript are random phases taken from a uniform distribution on the interval $-\pi$ to π and random amplitudes and population inversions.

So far, we have studied snapshots of the global behavior of the system at specific time instances. If we wish to verify that the above phenomena are robust under time evolution, we can measure the spatial coherence of these phenomena using a quantity called *local curvature* for each sublattice which may be calculated at each time instance by applying the discrete Laplacian DE on the spatial data of the amplitude of the electric field as follows:

$$DE_j(t) = |E_{j+1}(t)| + |E_{j-1}(t)| - 2|E_j(t)| \tag{40}$$

To quantify the spatial coherence of the observed patters we calculate separately the local curvatures DE_j^A and DE_j^B. Figure. 14 (left column) shows the spatio-temporal evolution of the absolute value of the local curvature in logarithmic scale corresponding to the states of Fig.14. In the fully synchronized case the local curvature is rescaled so that its maximum and minimum values are equal to zero, while in the case of arbitrary oscillations the local curvature oscillates in time. Figure. 14 (a) refers to the A sublattices and Fig. 14 (b) to the B sublattices respectively. The coexistence of the incoherent states with the coherent one for the two sublattices is evident.

In the case of small localized oscillations, the spatio-temporal evolution of the local curvature corresponding to the states of Fig.13 (right column) is plotted in Figure. 14 (right column) for (c) the A sublattice and (d) the B sublattice.

E. Variations of boundary conditions and detuning

In all of the analysis described so far, we have used periodic boundary conditions, thus it is important to investigate whether the same phenomena are observed in the case of open boundary conditions. Clearly, if one works with open ended arrays, lasers located at the boundaries are coupled to one neighbor, hence the average intensity of their output is lower than all the others. We have thus studied a system whose boundary dimers are oscillating while the remaining lattice is almost stationary. More precisely, we pump the boundary dimers with the rates $P_1 = P_{199} = 1.5$ and $P_2 = P_{200} = 0.4$, while for the remaining array we take $P_j^A = 1.5$ and $P_j^B = 1$, with all other parameters as in Fig. 13 (left column). The dimers on the boundaries are pumped with $P_1 = P_{199} = 1.5$ and $P_2 = P_{200} = 0.4$, while for the rest of the array $P_j^A = 1.5$ and $P_j^B = 1$. The results show that while the boundary dimers are oscillating, the local curvature of the remaining part is equal to zero and hence the LOCFP state of the system is not deformed.

In all our calculations so far, the detuning was set equal to zero. Extending our calculations to the case of non zero detuning, we calculated the spatio-temporal evolution of the local curvature for the amplitude of the electric fields of Fig.13 (left column), with detunings ω_j chosen from a normal random distribution with mean zero and standard deviation equal to $\sigma_\omega = 0.0075$. The coexistence of oscillatory and stationary states remains very similar as in Fig.14 (left column). For a proper choice of the amount of detuning one often chooses the mean value of the angular frequency of the relaxation oscillation of the uncoupled lasers $\omega_R = \sqrt{2P/T}$. However, since our system has three different pumping rates $P_a = 1.5$, $P_b = 0.4$ and $P_c = 1$, we use the mean value of the angular frequency of the relaxation oscillation as $\overline{\omega_R} = \frac{1}{N}\sum_{k=a,b,c}\sqrt{2P_k/T}$. Our numerical investigations show that, in order for oscillatory and stationary states to persist under the presence of detuning, the equality $\sigma_\omega \leq 0.1\overline{\omega_R}$ needs to be satisfied.

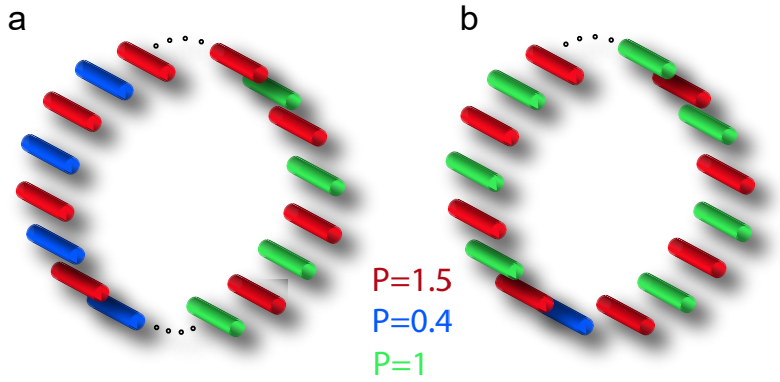

Fig. 12. Sketch of the overlap of the electric fields in coupled lasers of two A and B sublattices where network I has been furthermore separated into a two clusters where the elements of the left cluster are oscillating with large amplitude (LAO) while the right cluster supports localized oscillations close to the fixed point (LOCFP) (see Fig.13 (a) and (b)). Network II refers to the Fig.13 (d) and (e) where only the central dimer support LAO while the remaining system hold LOCFP.

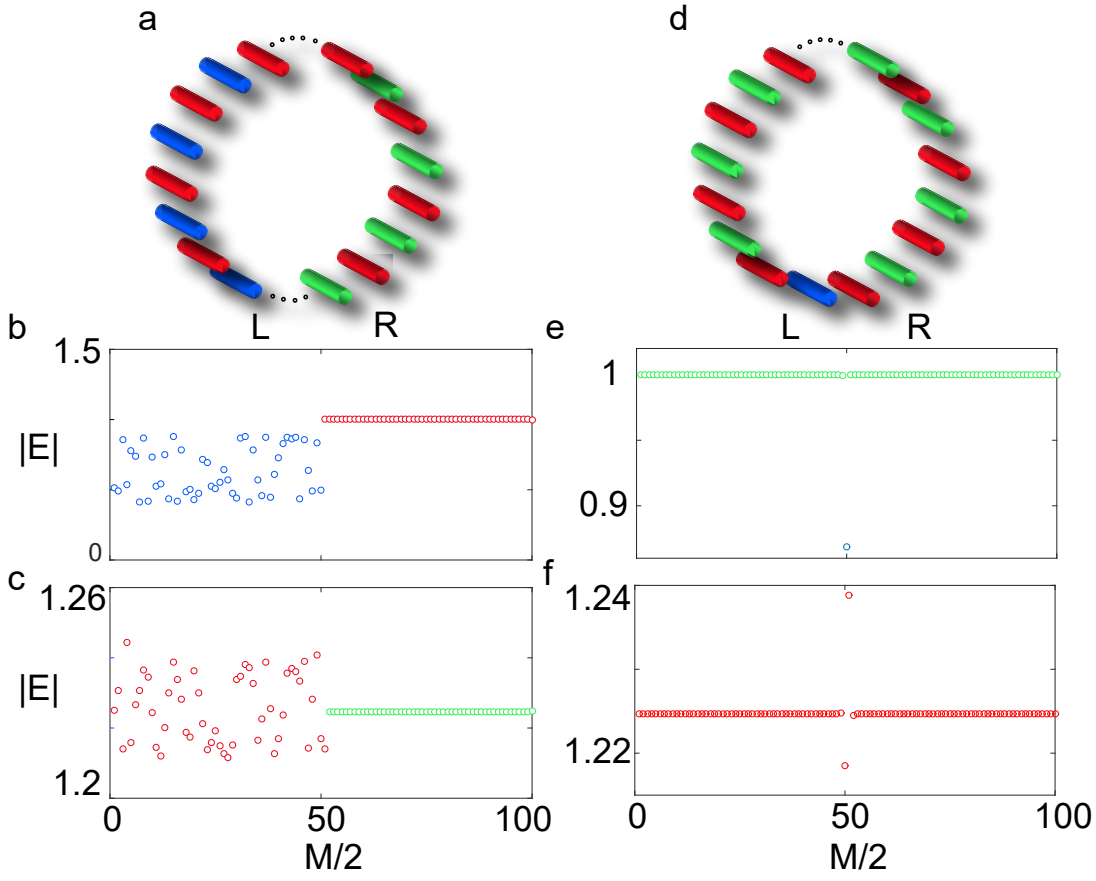

Fig. 13. Snapshots of the amplitude of the electric field in an array of M=200 lasers where, on the left column each sublattice array has 100 lasers and on the right has 100 lasers. (a) Depict the 100 lasers population of the A sublattice (S_A) which has been furthermore separated into a two clusters with the excess pump rate $P_j^A = 1$ for $j \in [1, M/2]$ and $P_j^A = 1.5$ for $j \in [M/2+1, M]$. The elements of the left cluster are oscillating with large amplitude (LAO) while the right cluster support localized oscillations close to the fix point (LOCFP). (b) The array of the B sublattice (S_B) with the extra pumping separation $P_j^B = 1.5$ for $j \in [1, M/2]$ and $P_j^B = 0.4$ for $j \in [M/2+1, M]$. In (d) only the dimer in the middle is separated from the rest with $P_{50}^A = 1.5$ and $P_{50}^B = 0.4$. In (e) and (f) we plot the amplitudes for each cluster and find that they are all of the LOCFP type. All other parameters as in Fig. 11.

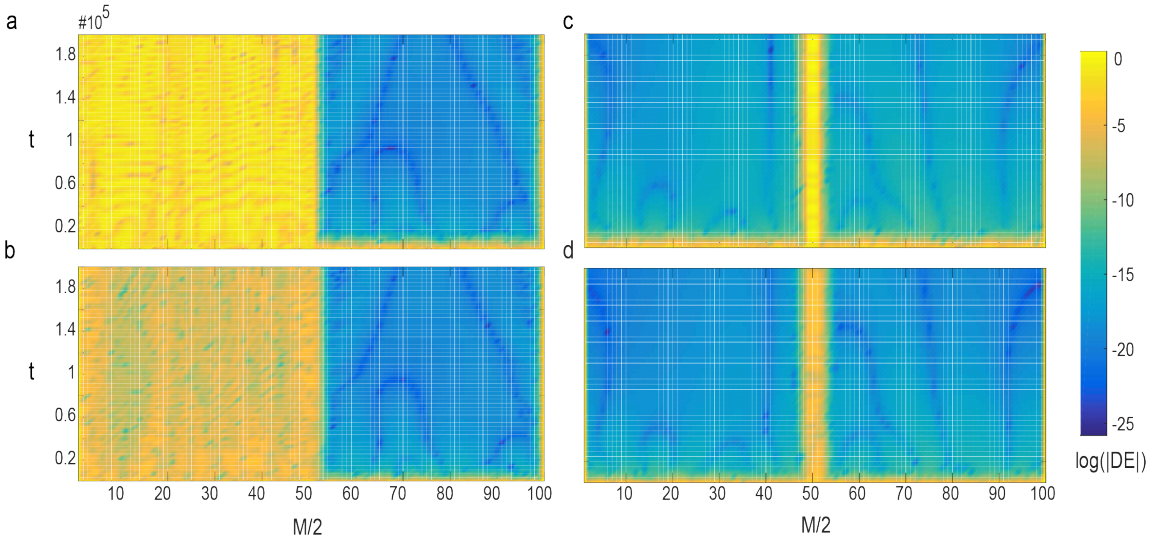

Fig. 14. Spatio-temporal evolution of the local curvature $|DE(t)|$ for the two sublattices A and B in a logarithmic scale where the left column refers to the parameter values as in Fig.13 (left column) and the right column depicts the local curvature of Fig.13 (right column). The top row refers to the A sublattices and the bottom to the B sublattices respectively. In the LOCEP case the log of a proper rescaling local curvature with its max and min is equal to minus infinity while in the case of LAO the log of local curvature oscillates in time close to zero. The proper pumping distribution and all the other parameters as in Fig. 13.

IV. CONCLUSIONS

In this MSc. Thesis we started with a preliminary study of synchronization and the formation of chimera states in a network of M = 100 Li- Sprott 4-dimensional nonlinear oscillators. We first carried out an analytical derivation of the approximate frequency and amplitude of the network's limit cycles (attracting periodic cycles) around the origin, in the state of complete synchronization, for low values of the coupling parameter d. Next, we carried out a numerical investigation focusing on the existence of synchronous as well as asynchronous oscillations that generate the fascinating phenomenon of chimera states in this model system as the coupling parameter of the problem is steadily increased and the initial conditions of the oscillators are judiciously chosen.

Our ultimate goal in this research, however, is to draw some conclusions about the oscillatory properties of a much more realistic and physically important system consisting of arrays of semiconductor laser dimers. In particular, viewing each dimer as a pair of coupled nonlinear oscillators, we first wished to understand analytically its steady states and their bifurcations to periodic solutions as one applies external pumping to the two lasers at different rates.

Based on the results for a single dimer, after determining parameter regions where stable limit cycles of synchronized oscillations arise, we turned to the study of an array (or network) of $M > 1$ coupled dimers to investigate whether synchronization occurs there also. Our aim was to avoid the occurrence of chaos, as well as chimera states, which after all constitute partial loss of synchronization, and see how reliable our photonic array is in terms of energy transmission and radiation.

In particular, we were interested to discover oscillatory phenomena in our *laser arrays* and use them as a tool to create a source of high-intensity radiation. This can be achieved by first coupling the lasers linearly in the form of two sublattices A and B, so that the dimers interact only with their nearest neighbors. The case of interactions with *groups* of neighbor elements, in the form of global coupling [22], is the result of an ongoing investigation, which is more difficult but very worthwhile, since it may turn out to be experimentally realistic in large laser arrays.

Separating the network in two clusters with equal pumping rates, so that the middle two dimers have different P_1, P_2, we observe cases where only the middle dimer undergoes large oscillations, while all its neighbors on the left and right execute very small oscillations in a state of "amplitude synchronization". However, when the two clusters have different pumping rates, the array exhibits a kind of "chimera state", where all dimers on the left population execute large oscillations, while the right population shows very low amplitude oscillations. An additional observation of synchronized behavior is the case where the phase difference between the amplitude of the electric fields of the two lasers of the dimers that belong to the A sublattice are synchronized in frequency but out of phase, while those of the B sublattice are practically stationary very close to their equilibrium states.

In conclusion, we have found that, close to the unstable fixed points, small localized oscillations coexist with large amplitude oscillations for large arrays of active photonic dimers driven externally with differential pumping rates. Different realizations on pumping rates generate these states and this asymmetry has the same impact on the carrier densities, corresponding to values that are above and below threshold so that the respective electric fields experience gain and loss. These dynamical behaviors are robust in different initial conditions, boundary conditions and system size. Moreover, a systematic study in random optical frequency detuning shows that these phenomena are stable even under a large standard deviation of randomness. The ability to control the dynamics of this system through the pumping rates, which are the most conveniently accessible control parameters in chip scale diode systems, may have multiple technological applications.

In closing, we would like to mention is another very interesting phenomenon that arises in networks of coupled nonlinear oscillators called *Kuramoto self-synchronization transition.* [2]. It is applicable when nonidentical *phase* oscillators with different frequencies are coupled. When two oscillators have very close frequencies they easily synchronize. As a result, their contribution to the mean field at the frequency of these synchronous oscillations increases. This increased component of the driving force naturally entrains other elements that have close frequencies and this leads to

the growth of synchronized clusters and to a further increase of the component of the mean field at a certain frequency [2]. So, based on these observations, we plan to extend our goals in the future and also investigate the occurrence of Kuramoto self-synchronization in photonic arrays.

As an extension of this research, we propose to study arrays of semiconductor laser dimers with different types of intra–dimer coupling to investigate the arrays' reliability in terms of energy transmission and secure communication. Also, it will be very interesting to compare results from different types of inter–dimer array coupling. Thus, our future goal will be to try to better understand these oscillatory properties so we can suggest specific applications in the field of photonics that can be tested experimentally. Our *Deliverables* will be to complete the work of this MSc thesis and be able to write a paper describing the results of our research that can be accepted for publication in an international journal.

REFERENCES

[1] Strogatz, S(1993). Nonlinear Dynamics and Chaos, 1st ed., vol. 1., Reading, Massachusetts.

[2] Pikovsky A, Kosenblum M, Kurths J, 2001, Synchronization. A Universal Concept in Nonlinear Sciences, New York, Cambridge University Press.

[3] J. C. Sprott (2001), "Chaos and Time Series Analysis", Oxford University Press, Oxford, England.

[4] Dudkowski D, Maistrenko Y, Kapitaniak T. Occurence and stability of chimera states in coupled externally excited oscillators. Chaos: An Interdisciplinary Journal of Nonlinear Science. 2016;26:116306.

[5] Mishra A, Saha S,Roy PK, Kapitaniak T, Dana SK. Multicluster oscillation death and chimeralike states in globally coupled Josephson Junctions. Chaos: An Interdisciplinary Journal of Nonlinear Science. 2017;27:023110.

[6] Wojewoda J, Czolczynski K, Maistrenko Y, Kapitaniak T. The smallest chimera state for coupled pendula. Scientific reports. 2016;6.

[7] Rakshit S, Bera BK, Perc M, Ghosh D. Basic stability for chimera states. Scientific reports. 2017;7.

[8] T.Bountis, Kanas VG, Hizanidis J, Bezerianos A. Chimera states in a two-population network of coupled pundulum-like elements. Eur Phys J Spec Top, 2014;223:721-8.

[9] Y.Kominis, V.Kovanis, T.Bountis, "Controllable asymmetric phase-locked states of the fundamental active photonic dimer," Physical review A 96, 043836 (2017).

[10] J.Shena, J.Hizanidis, V.Kovanis, G.P.Tsironis "Turbulent chimeras in large semiconductor laser arrays," Scientific reports 7, 42116 (2017).

[11] Li C, Sprott J.C. Coexisting hidden attractors in a 4-D simplified Lorenz system. International Journal of Bifurcation and Chaos. 2014;24:1450034.

[12] Parastesh F, Jafari S, Azarnoush H, Hatef B, Bountis T, "Imperfect Chimera in a ring of four dimentional simplified Lorenz systems," Chaos,Solitons and Fractals 110 (2018), 203-208.

[13] D. G. Aranson, G.B. Ermentrout, and N. Kopell, Amplitude response of coupled oscillators, Physica D (Amsterdam) 41, 403 (1990).

[14] Zehnl V., Theoretical model for coupled solid-state lasers, Phys. Rev. A 62, 33814(2000).

[15] A. Hohl, A. Gavrielides, T. Erneux, and V. Kovanis, "Localized Synchronization in Two Coupled Nonidentical Semiconductor Lasers," Phys. Rev. Lett. 78, 4745 (1997).

[16] S.S. Wang and H.G. Winful, "Dynamics of phase-locked semiconductor laser arrays," Appl. Phys. Lett. 52, 1774-1776 (1988).

[17] M.C.Soriano, J. Garcia-Ojalvo, C.R. Mirasso, and I.Fischer, Complex photonics: Dynamics and applications of delay-coupled semiconductors lasers, Rev.Mod.Phys.85,421(2013).

[18] Y.Kominis, V. Kovanis, and T. Bountis, Spectral signatures of exceptional points and bifurcations in the fundamental active photonic dimer, Physical review A 96, 053837 (2017).

[19] Y. Kominis, Kent D. Choquette, A. Bountis and V. Kovanis, "Exceptional Points in Two Dissimilar Coupled Diode Lasers", Appl. Phys. Lett. 113, 081103 (2018). https://arxiv.org/pdf/1806.01098.pdf

[20] Y. Kominis, K. D. Choquette, V. Kovanis, and A. Bountis, "Antiresonances and Ultrafast Resonances in Coupled Twin Photonic Oscillator", IEEE Photonics (January 2019). https://arxiv.org/abs/1808.03760

[21] Y. Kominis, Th. Erneux, A, Bountis, Vassilios Kovanis, "Controllable Limit Cycles of a Widely Tunable Photonic Oscillator", preprint (2019).

[22] J. Shena, Y. Kominis, A. Bountis and Vassilios Kovanis "Controlling localized patterns in coupled array of semiconductor lasers", preprint (2019).

[23] H. G. Winful and S. S. Wang, "Stability of phase locking in coupled semiconductor laser arrays", Appl. Phys. Lett. 53, 1894 (1988).